Chapter 8

Design and Simulation of Ultra Compact Tesla Transformer

–Ankan Basak

Pulsed power sources, as prevalent in its history are large devices with huge footprint. Researchers and scientists made efforts to reduce this particular drawback of pulsed power sources to unlock its potential in several societal and mobile applications. This opened the doors of portable dynamic X-ray sources to a vast application in the field of geology and gemology [1]. All of these new designs had two major driving factors. Firstly, the energy density of the capacitors has increased by many folds making the primary energy storage much more compact. Secondly, the pulse duration of the output voltage pulse was decreased tremendously, which in turn decreases the holding time of the voltage, as result insulation was improved.

8.1. Introduction

Pulse power systems are useful to drive High Power Microwave (HPM) [2] and Flash X-ray (FXR) [3] devices. Tesla transformer is a part of pulse power system, which finds its application to charge Pulse Forming Line from the energy stored in the primary capacitor bank. This transmission line is discharged to a load with high voltage and high current of magnitude several kilovolts and kilo amps respectively with few tens of nanoseconds pulse duration. Tesla transformer is used where high repetition rate is required [4]. An alternate way to address this problem is to use Marx Generator, however, conventional Marx Generators cannot go beyond 10 Hz repetition rate, as it is made of several spark gap (SG) switches, and due to slow restoration of ions to its parent atoms after a spark gap is triggered. The Tesla transformer needs only a single spark gap switch as compared to large number of SGs used in a Marx Generator, therefore can produce a fast rise time pulse and thereby practically more reliable. In addition to this only one single SG offers more life time, making it attractive over other pulsed sources.

8.2. Theory and operation of Tesla Transformer

A typical Tesla Transformer consists of two inductively coupled damped resonance circuits. The primary capacitor is initially charged which is allowed to discharge by a switch S through a low inductive coil (L_1). This inductive coil is magnetically coupled to a multi-turn secondary of higher inductance (L_2). Magnetic flux linkage between the two coils generates a magnified voltage on the secondary. One terminal of the secondary is connected to the ground and other terminal is connected to the secondary capacitor (C_2). When the switch S is closed current starts to flow in the primary circuit at a frequency corresponding to natural frequency of determined by the primary capacitance (C_1) and the primary inductive coil (L_1). The oscillations of the magnetic field are coupled to the secondary side of the transformer. A part of energy is transferred to the secondary side which charges the secondary capacitor at a much higher voltage. The schematics are shown in the Figure 8.1.

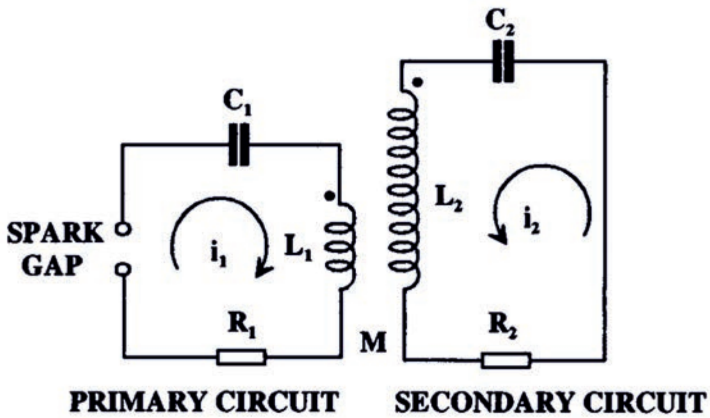

Figure 8.1. Circuit of Tesla transformers [5].

As the primary and secondary side are tuned in such a way to resonate at same frequency we have,

$$L_1 C_1 = L_1 C_2 \tag{8.1}$$

Applying Kirchhoff's Voltage Law in both the loops we get [5],

$$R_1 I_1 + \frac{1}{C_1}\int I_1 dt + L_1 \frac{di_1}{dt} + M\frac{di_2}{dt} = 0 \tag{8.2}$$

$$R_2 I_2 + \frac{1}{C_2}\int I_2 dt + L_2 \frac{di_2}{dt} + M\frac{di_1}{dt} = 0 \tag{8.3}$$

Analytical solution for above two equations are possible only if the losses in primary and secondary circuits are ignored i.e. R_1 and R_2 are zero. Then the voltage V_2(t) across C_2 can be represented as [3],

$$\mathrm{V_2(t)} = \frac{2k}{\sqrt{(1-T)^2 + 4kT^2}}\sqrt{\frac{L_2}{L_1}}\sin(\frac{w_2 - w_1}{2}t)\sin(\frac{w_2 + w_1}{2}\mathrm{t}) \tag{8.4}$$

Where,

$$k = \frac{M}{\sqrt{L_1 L_2}} \qquad \omega_i = \frac{1}{\sqrt{L_i C_i}} \quad i = 1,2 \qquad T = \frac{\omega_1^2}{\omega_2^2}$$

$$\mathrm{w}_1 = \omega 2\sqrt{\frac{(1+T) - \sqrt{(1-T)^2 + 4k^2 T}}{2(1-k^2)}} \tag{8.5}$$

$$\mathrm{w}_2 = \omega 2\sqrt{\frac{(1+T) + \sqrt{(1-T)^2 + 4k^2 T}}{2(1-k^2)}} \tag{8.6}$$

Where k is coupling co-efficient of the transformer and ω_1 and ω_2 are the angular resonance frequencies of the un-coupled primary and secondary circuits, respectively. It is reported in the literature that for coupling co-efficient $k>0.8$ the maximum voltage at the output is obtained in the first peak where for coupling co-efficient k between 0.5 and 0.7 the maximum voltage occurs at second peak. Which is eventually the case for air cored Tesla Transformers. Implementing semiconductor switches was the primary motto of this work. Which imposes stringent measures on the maximum permissible value of primary peak current (I_{1max}) and $(di/dt)_{max}$. These values are expressed as [6],

$$I_{1_{max}} = \frac{V_1\sqrt{C_1}}{2\sqrt{(1-k)L_1}}[1 + \sqrt{\frac{1-k}{1+k}} sin\left(\frac{\Pi}{2}\sqrt{\frac{1-k}{1+k}}\right)] \tag{8.7}$$

$$\left(\frac{di}{dt}\right)_{max} = \frac{V_1}{(1-k^2)L_1} \tag{8.8}$$

Maximum achievable output from a secondary of the Tesla Transformer can be optimised by optimising the following expression [3],

$$G = \left(\frac{V_2(t)}{V_1}\right)\max = \frac{2k}{\sqrt{(1-T)^2 + 4kT^2}} GL \tag{8.9}$$

Where,

$$G_L = \sqrt{\frac{L_2}{L_1}} \tag{8.10}$$

The gain G is achieved when the sine terms in the expression of $V_2(t)$ is ± 1 simultaneously, which yields,

$$\frac{w_2+w_1}{2}t = \frac{\Pi}{2} + m\Pi \quad \text{and} \quad \frac{w_2-w_1}{2}t = \frac{\Pi}{2} + n\Pi \tag{8.11}$$

Where m and n are positive integers, without losing generality we can assume $n = 0$, then we have,

$$\frac{w_2}{w_1} = \frac{1+m}{m} \tag{8.12}$$

Combining Eqs. (8.5), (8.6) and (8.12) we get,

$$k = \sqrt{\frac{\alpha^2(1+T)^2 - (1-T)^2}{4T}} \tag{8.13}$$

Here,

$$\alpha = \frac{1+2m}{1+2m+2m^2} \tag{8.14}$$

Eliminating k from Eqs. (8.9) and (8.13) we get,

$$G = \left(\frac{V2(t)}{V1}\right)\max = \sqrt{\frac{\alpha^2(1+T)^2 - (1-T)^2}{\alpha^2 T(1+T)^2}}\, G_L \tag{8.15}$$

The variation of G/G_L with tuning ratio T is shown in the Figure 8.2.

As, $G_L = \sqrt{\frac{L_2}{L_1}}$ we can rearrange it and write it as,

$$G_L = \sqrt{T}\sqrt{\frac{C_1}{C_2}} \tag{8.16}$$

If we tune by changing inductances L_1 or L_2 and keeping capacitances fixed, then gain,

$$G = \sqrt{\frac{\alpha^2(1+T)^2 - (1-T)^2}{\alpha^2 T(1+T)^2}}\sqrt{T}\sqrt{\frac{C_1}{C_2}} = GT\sqrt{\frac{C_1}{C_2}}\ \sqrt{T} = K1\sqrt{\frac{C_1}{C_2}} \tag{8.17}$$

Where $G_T = \sqrt{\frac{\alpha^2(1+T)^2-(1-T)^2}{\alpha^2 T(1+T)^2}}$ and $K_1 = G_T\sqrt{T}$

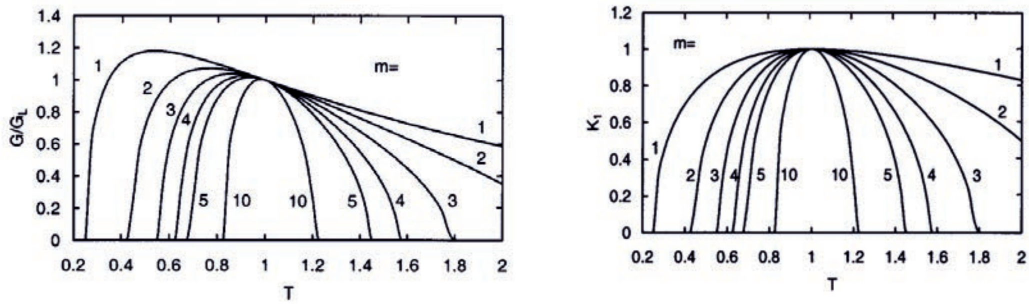

Figure 8.2. G/G_L gain vs. tuning ratio (T) (left) and K_1 gain vs. Tuning ratio T for different m values (right) [5].

Similarly, if we tune by changing capacitance C_1 or C_2 by keeping L_1 and L_2 constant, the maximum achievable voltage at the secondary for energy of E_0 stored in the primary capacitor is,

$$V_2 = \sqrt{\frac{2E_0}{C_1}}\, G_T \sqrt{\frac{L_2}{L_1}} \tag{8.18}$$

This can be rearranged as follows,

$$V_2 = \sqrt{2E_0}\, G_T \sqrt{\frac{L_2}{L_1}} \sqrt{\frac{L_1 T}{L_2 C_2}} \propto G_T \sqrt{T} \tag{8.19}$$

Irrespective of the value of m, it is evident from the Figure 8.2 that optimum performance of Tesla transformer is achieved for a tuning ratio T = 1. That is,

$$L_1 C_1 = L_1 C_2 \tag{8.20}$$

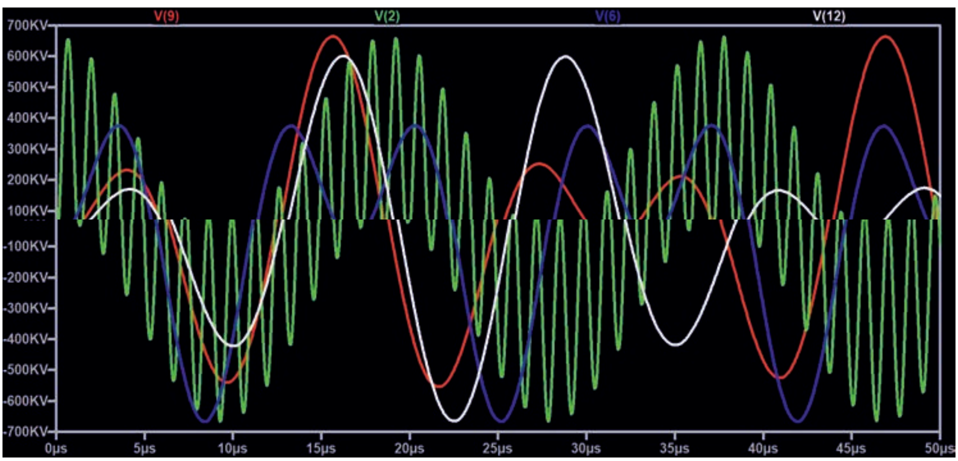

Figure 8.3. Figure shows output voltage waveform for k = 0.99 (green), k = 0.6 (blue), k = 0.38 (red) and k = 0.28 (white).

In eqn. (8.5) we put $T = 1$, and we get $k = \alpha$. So for $T = 1$ we have,

$$k = \frac{1 + 2m}{1 + 2m + 2m^2} \text{ where m } = 1, 2, 3 \ldots \tag{8.21}$$

So the values of k for which optimum performance is achieved are k = 0.6, 0.38, 0.28 . . .

Energy efficiency of a Tesla Transformer is given by,

$$\eta = \frac{C_2 V_2^2}{C_1 V_1^2} = T\, G_T \tag{8.22}$$

So 100% energy transfer is possible in Tesla Transformers when $T = 1$ and $k = 0.6, 0.38, 0.28$. Figure 8.3 shows the output voltage plots for various coupling co-efficient. It is evident from the figure that peak voltage appears at $(m+1)^{th}$ peak. For $k = 0.99$ the peak voltage appears at the first peak, which relaxes the insulation requirement, hence it is recommended to have a coupling co-efficient greater than 0.9 for all practical applications.

In the above analysis it was assumed that the primary and secondary sides of the transformer are of zero resistance. But due to skin effect, proximity effect and equivalent series resistance (ESR) of primary capacitor some resistance comes into picture. Some studies available in literature [6] to model this type of non-ideal system. Let Q_1 and Q_2 are the quality factors of the primary and secondary side of the transformer respectively,

$$Q_1 = \frac{L_1 \omega_1}{R_1} \quad \text{and} \quad Q_2 = \frac{L_2 \omega_2}{R_2}$$

Then an approximate expression for the voltage in secondary is given by,

$$V_2(t) = \frac{V_0}{2} \sqrt{\frac{L_2}{L_1}}\, e^{\left(\frac{-t}{\tau}\right)} \left[\cos\left(\frac{\omega t}{\sqrt{1-k}}\right) - \cos\left(\frac{\omega t}{\sqrt{1+k}}\right)\right] \tag{8.23}$$

Where, $\tau = \frac{4 Q_1 Q_2 (1-k^2)}{\omega (Q_1 + Q_2)}$, Where $\omega_1 = \omega_2 = \omega$

8.3. B-H curve

In order to develop a High coupling open magnetic core Tesla transformer, it is imperative to use a core with high permeability and to withstand high magnetic flux density. To meet these criteria an ideal design choice will be to go for a core with very high saturation flux density, high relative permeability even at high frequencies. On top of that, core losses should be least at these conditions.

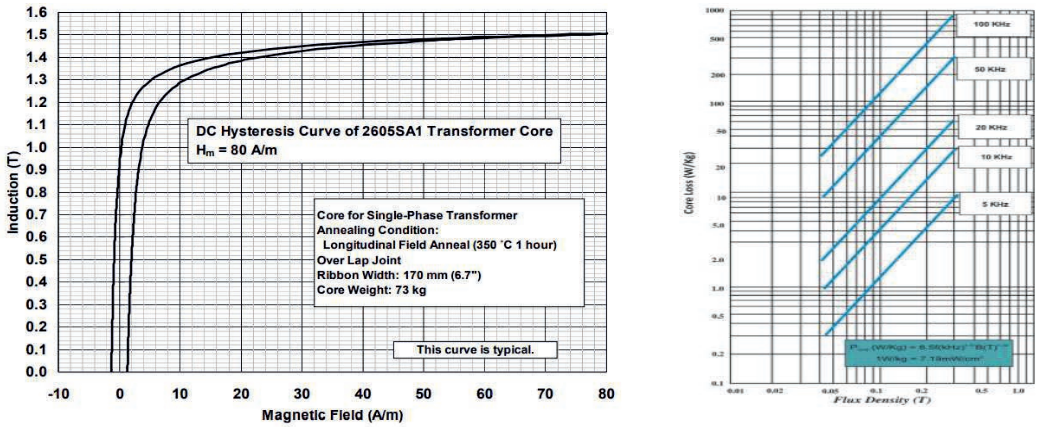

Figure 8.3. Hysteresis loop of Metglas 2605SA1 [8] (left) and core loss vs. magnetic flux density at different operating frequencies [9] (right).

Metglas 2605SA1 proved itself as a suitable candidate for this kind of applications [7]. With an aim to reduce losses and introduce anisotropy in the material, longitudinal field annealing was done at high temperature, influenced by a high magnetic field. Various data relating to Metglas is depicted in Figure 8.3.

8.4. Design and Simulations

The design specifications are mentioned in Table 8.1.

Table 8.1. Design specifications of the transformer.

Input voltage	Pulse width	Output current	Rise time	Output voltage
1 kV	5 ns	3.3 kA	600 ps	200 kV

$$V \times I \times t = \frac{1}{2} \times C \times V_{charging}^2 \tag{8.24}$$

From Eq.(8.24) the required capacitance to be charged is calculated to be 37.5 pF. Here we assumed that a co-axial transmission line will be charged by Tesla transformer to 400 kV which when discharged to a matched load will generate 200 kV at the output. The capacitance of a transmission line is given by,

$$C_{Line} = \frac{2\Pi\, \mathcal{E}_0\, \mathcal{E}_r \mathrm{l_T}}{\ln\left(\frac{r_o}{r_i}\right)} \tag{8.25}$$

This line is discharged to a load through a high voltage gas switch. For maximum power transfer, the load impedance has to be matched with the line impedance. So the matched impedance of this type of pulsed power generators is,

$$Z_{Load} = \frac{60}{\sqrt{\mathcal{E}_r}} \ln\left(\frac{r_o}{r_i}\right) \tag{8.26}$$

From a line of length l_T we can get a pulse of duration t_p which is given by,

$$t_p = \frac{2l_T\sqrt{\mathcal{E}_r}}{c} \tag{8.27}$$

For avoiding a bulk breakdown inside the insulating medium, electric field inside the region has to be less than the breakdown voltage of the medium. This gives another constraint as shown below.

$$E_{BD} \geq \frac{V}{r_i \ln\left(\frac{r_o}{r_i}\right)} \tag{8.28}$$

SF_6 gas will be used as insulating gas inside the transformer so the relative permittivity ($\mathcal{E}_r$) will be unity and its breakdown strength (E_{BD}) will be greater than 120kV/cm for µs pulses. This gives us,

$$\ln\left(\frac{r_o}{r_i}\right) = 1, or\ r_o = 2.3r_i$$

The inner radius is given by,

$$r_i = \frac{V}{E_{BD}} = \frac{400}{120} = 3.33\ cm$$

So the outer radius is given by $r_o = 3.35 \times 2.3 = 7.705\ cm$.

From Eq.(8.27) the length of the pulse forming line is given by, $l_T = 75\ cm$.

The core of the transformer acts as pulse forming line; in that case the performance of the transformer is largely dependent on the ability of the core material to withstand high magnetic flux density without getting saturated. So for pulsed transformers we have,

$$\frac{V_{2max}T}{2} = N_2 B_{sat} A \tag{8.29}$$

By making use of Metglas 2605SA1 as core material which has high saturation magnetic flux density of 1.56 T, the cross sectional area required to avoid core saturation for a 400 kV, 5 µs charging is given by 961 mm^2.

Various inductance of this type of co-axial transformer is given by [10],

$$\text{Magnetising inductance } L_u = \frac{\Pi}{2}\mu_0 N_1^2 \frac{l_t - l_k}{\ln\beta} \tag{8.24}$$

$$\text{Leakage inductance Ls } = \frac{\Pi}{3}\mu_0 N_1^2 \frac{r_o^2}{l_k}\frac{(\beta-1)(2\beta+1)}{\beta^2} \tag{8.25}$$

And

$$k = \sqrt{1 - \frac{L_S}{L_u}} = [1 - \frac{2}{3}\frac{r_o^2}{l_k(l_T - l_k)}\frac{(\beta-1)(2\beta+1)}{\beta^2}\ln\beta]^{1/2} \tag{8.26}$$

Where $\beta = r_o/r_i$

$$L_1 = L_u + \frac{L_S}{2} \text{ and } L_2 = \frac{N_2^2}{N_1^2}L_1 \tag{8.27}$$

Table 8.2. Various dimensions chosen for the transformer core.

Length of the core(mm)	450 mm
Length of the winding(mm)	300 mm
Inner dia. of the outer core(yoke)	180 mm
Outer dia. of the inner core	67 mm
Number of turns in the secondary	610
Core cross sectional area of the inner core	1800 mm^2
Outer core cross sectional area	1200 mm^2

As illustrated in the model considered for simulation shown in the Figure 8.7, the Metglas (in blue) is actually embedded in stainless steel (in gray), to provide structural support for the core. The dimensions of the model considered are shown in Table 8.2 and various inductances as simulated and calculated are shown in Table 8.3.

To make the transformer compact the inner core of the transformer is used as the central conductor of the PFL and the yoke is used as the outer conductor. Also SF_6 gas will be used as a dielectric to insulate between central conductor and outer conductor. Relative permittivity of SF_6 is 1. The capacitance of the said structure was calculated in CST. The electric field pattern and magnetic field pattern is shown in the Figure 8.4. The capacitance was calculated was found to be 27 pF.

Table 8.3. Calculated and simulated values of various parameters of the transformer.

Name of the parameter	**Value of the parameter(calculated)**	**Value of the parameter(simulated)**
Primary inductance (nH)	330	364
Secondary inductance (mH)	146.8	168
Coupling co-efficient	0.9	0.92

Circuit simulation is carried out in LTSpice to obtain the PFL voltage waveform. The circuit and the output voltage is shown in the Figure 8.5. The peak voltage of the PFL was around 500 kV at a time instant of 2 µs. Results are shown in Figure 8.5. When the voltage of the PFL will reach its maximum the output spark gap will start to conduct and power will be delivered to a load of 60 Ω. The spark gap along with the line is designed in CST and simulated for the output pulse. The results are depicted in Figure 8.6 for a 1 V of PFL charging. The figure shows that half of the voltage is obtained at the load for time duration of 5 ns.

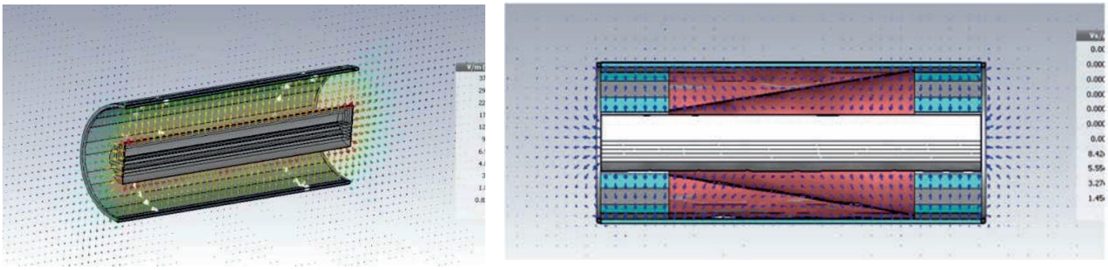

Figure 8.4. Electric field Pattern inside the structure (left) and Magnetic Field pattern inside the structure (right).

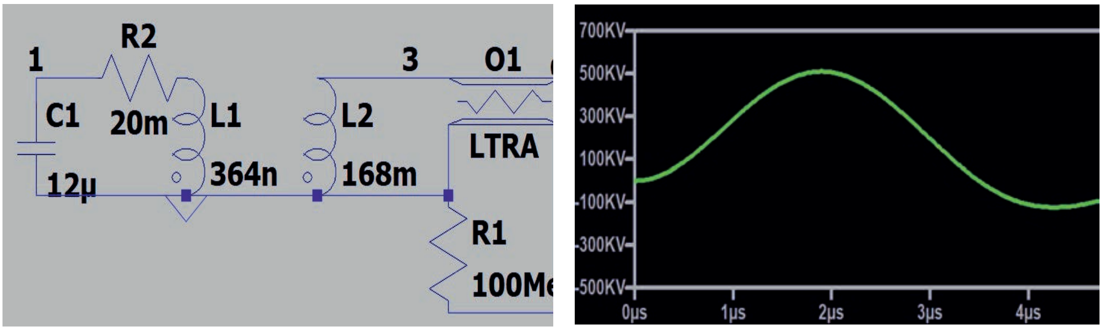

Figure 8.5. Circuit considered for simulation (left) and Simulated voltage of the PFL (right).

8.5. Conclusion

A compact Tesla transformer was simulated capable of delivering 250 kV at a load of 60 Ω for a charging of 1 kV at its primary. The transformer is designed [9] in such a way that the coupling co-efficient is greater than 0.9. This ensures the required output voltage to occur at first peak [5]. The transformer first charges the PFL with 500 kV then the spark gap attached to it breaks down to deliver half of the voltage i.e. 250 kV voltage pulse for a duration of 5 ns to the load. The magnetic field and electric field plots are shown. Various measures are taken to mitigate effects like electrical breakdown, magnetic core saturation.

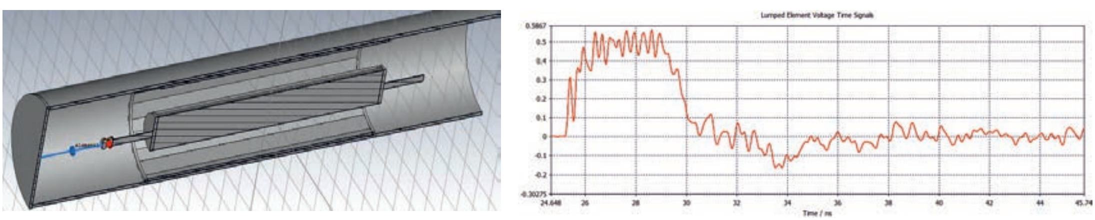

Figure 8.6. Structure considered for simulation of output voltage pulse (left) and Simulated voltage pulse on a 60 Ω load for 1 V of PFL charging in Y axis with time in the X axis (right).

References

[1] Mesyats, G. A., V. G. Shpak, M. I. Yalandin, and S. A. Shunailov. "RADAN-EXPERT portable high-current accelerator." In Digest of Technical Papers. Tenth IEEE International Pulsed Power Conference, vol. 1, pp. 539-543. IEEE, 1995.

[2] Roy, Amitava, Rakhee Menon, S. Mitra, Senthil Kumar, Vishnu Sharma, Archana Sharma, K. V. Nagesh, and D. P. Chakravorthy. "High power microwave generation from KALI 5000 pulse power system." In 2011 IEEE Pulsed Power Conference, pp. 387-390. IEEE, 2011.

[3] Menon, Rakhee, Amitava Roy, S. Mitra, Archana Sharma, J. Mondal, K. C. Mittal, K. V. Nagesh, and D. P. Chakravarthy. "Generation and dose distribution measurement of flash X-ray in KALI-5000 system." Review of Scientific Instruments 79, no. 10 (2008): 103301.

[4] Bykov, N. M., A. V. Gunin, S. D. Korovin, and Yu D. Korolev. "Operating features of a high-voltage spark gap switch with gas blow normal to the breakdown path in a repetitively pulsed mode." Instruments and Experimental Techniques 51 (2008): 838-845.

[5] Denicolai, Marco. "Optimal performance for Tesla transformers." Review of Scientific instruments 73, no. 9 (2002): 3332-3336.

[6] Liu, Yunlong, Li Lee, Yu Bing, Yafeng Ge, Wen Hu, and Fuchan Lin. "Resonant charging performance of spiral tesla transformer applied in compact high-voltage repetitive nanosecond pulse generator." IEEE Transactions on Plasma Science 41, no. 12 (2013): 3651-3658.

[7] Pecastaing, Laurent, Marc Rivaletto, Antoine Silvestre De Ferron, Romain Pecquois, and Bucur M. Novac. "Development of a 0.6-MV ultracompact magnetic core pulsed transformer for high-power applications." IEEE Transactions on Plasma Science 46, no. 1 (2017): 156-166.

[8] https://metglas.com/wp-content/uploads/2021/06/2605SA1-Magnetic-Alloy-Updated.pdf

[9] https://www.uaml.in/amorphous-c-cores.php

[10] Jeong, Young-Kyung, Dong-Gi Youn, and Moon-Qee Lee. "A study on optimization of compact high-voltage generator based on magnetic-core Tesla transformer." Journal of Electrical Engineering and Technology 9, no. 4 (2014): 1349-1354.